Effects of diffusion on interfacial fracture of gold-chromium hybrid microcircuit films

N.R. MOODY[1,*], D.P. ADAMS[2], D. MEDLIN[1], T. HEADLEY[2], N. YANG[1] and
A. VOLINSKY[3]

[1]*Sandia National Laboratories, Livermore, CA 94551-0969, U.S.A. (*Author for correspondence:
E-mail: nrmoody@sandia.gov)*
[2]*Sandia National Laboratories, Albuquerque, NM 87185-0959, U.S.A.*
[3]*Motorola, Mesa, AZ 85202, U.S.A.*

Abstract. In this study, the effects of diffusion on gold-chromium film durability was determined from interfacial fracture energy measurements on laboratory samples aged to simulate long term service. The samples were prepared by sputter deposition of gold films and chromium adhesive layers on sapphire substrates. Some films were left in the as-deposited condition while others were given an accelerated age to drive the chromium off the interface and into the gold film. Stressed overlayers and nanoindentation were then used to induce interfacial delamination and blister formation from which interfacial fracture energies were determined using mechanics-based models. These tests showed that the fracture energies for interfacial failure of the as-deposited and annealed films occurred near 1.3 J m^{-2} even when diffusion had driven all chromium into solution. These results clearly demonstrate that chromium in solution is as effective in promoting adhesion as continuous chromium adhesive layers.

Key words: Gold films, gold-chromium films, interfacial fracture, nanoindentation, stressed overlayers.

1. Introduction

Interface structure and composition are important factors controlling the performance and reliability of thin film devices (Mittal, 1976; Mattox, 1973). They are particularly important in gold-chromium hybrid microcircuits which consist of an alumina substrate, a thin chromium layer for adherence, and a gold layer for conductance to connect components on the microcircuit (Munitz and Komem, 1976; Thomas and Haas, 1972; Rairden et al., 1971). During post deposition annealing, lead-frame bonding and service at elevated temperature, diffusion and segregation change the composition and structure of the films and interfaces (Munitz and Komem, 1976, 1980; Thomas and Haas, 1972; Rairden et al., 1971; George et al., 1990). This has caused significant concern as to the long-term effects of chromium migration on film performance and durability and has motivated numerous studies on diffusion processes and their effects on film properties and performance. These tests have repeatedly shown that chromium diffusion continues until the chromium adhesion layer has been depleted. Although chromium diffusion and depletion are critical issues in long-term durability of devices with these films, the effects of these processes on film adhesion are not well defined due to limitations in test techniques (Kriese et al., 1998, 1999; Moody et al., 1998a; Volinsky et al., 2002a).

Traditional fracture test techniques use a sandwich configuration where a film is deposited on each of two substrates and diffusion bonded under high pressure at elevated temperature (Cao and Evans, 1989; Charalambides et al., 1989; Suo and Hutchinson, 1989). The

bonding process can lead to changes in the composition and microstructure of the film as well as the interface. It can also lead to greater adhesion, higher fracture energies, and more plastic deformation than observed in as-deposited films. In contrast, peel tests preserve the as-manufactured character of the films but give fracture energies dominated by plastic energy contributions as the film is bent (Wei and Hutchinson, 1998). These measurements are made even more difficult for gold films as extensive plasticity limits the stress that can be applied at the film-substrate interface (Kriese *et al.*, 1999).

The work of Bagchi et al. (1994, 1996), and more recent work by Bahr et al. (1997) and Kriese and coworkers (1998, 1999) show that these limitations can be overcome by deposition of a hard, highly stressed overlayer. This overlayer applies a uniform stress to the ductile films while constraining out-of-plane plasticity (Bagchi et al., 1994; Bagchi and Evans, 1996; He et al., 1996). It is typically a refractory metal deposited at a relatively low temperature so as not to alter the composition and structure of the underlying film or interface of interest, yet at a temperature high enough to bond with the surface of the ductile metal film. (Kriese et al., 1998, 1999). When combined with nanoindentation, the overlayer and nanoindentation stresses trigger delamination and blister formation from which fracture energies can be determined. We used this approach to study how changes in composition and structure affect susceptibility to interfacial fracture of gold-chromium films used in hybrid microcircuits. The results clearly show that chromium promotes adhesion. More importantly, the results show that chromium in solution is as effective in promoting adhesion as a continuous chromium layer.

2. Materials and procedure

In this study, thin gold and gold-chromium films were sputter deposited onto polished single crystal (0001) sapphire substrates using a d. c. magnetron sputtering unit. The substrates were prepared by ultrasonic cleaning in acetone for ten minutes, in ethyl alcohol for five minutes, and then in 1 M HCl for five minutes. This was followed by rinses with deionized water and nitrogen gas. They were then transferred to the deposition chamber and heated to 700 °C in vacuum for five minutes to drive off moisture and cooled to 250 °C. With the vacuum at a base pressure of 1.3×10^{-5} Pa (10^{-7} Torr), the films were deposited on the substrates using chromium and gold targets, and argon as the carrier gas. Chromium was first deposited on three substrates to a thickness of 6 nm. This was followed by gold deposition to a thickness of 200 nm. Both were deposited at a nominal rate of 0.3 nm s^{-1} at 180 W. The gold-chromium film samples were then divided into three groups. One sample was left in the as-deposited condition. A second sample was heated at 400 °C for 2 hours in air at which point the continuous chromium layer had begun to come off the sapphire interface in many regions. This sample is referred to as partially annealed. The third sample was then heated at 400 °C for 8 hours in air at which point the continuous chromium layer had been completely reduced to a solid solution of gold and chromium. This sample is referred to as fully annealed. During heating, chromium had diffused through the gold film to the surface forming Cr_2O_3 upon exposure to air. This oxide was removed using a solution of ceric ammonium nitrate.

Following nanoindentation testing for mechanical properties, a tantalum nitride (Ta_2N) overlayer was deposited on all films to provide a uniform compressive stress for fracture testing. Deposition was accomplished by placing the gold and gold-chromium films in the sputter deposition chamber and heating to 170 °C in vacuum to drive off moisture. Cleaning

was completed with an RF backsputter to remove contaminants from the surface. Within a vacuum system having a base pressure of 1.3×10^{-5} Pa (10^{-7} Torr), the tantalum nitride films were deposited at a rate of 0.3 nm s^{-1} to a thickness of 430 nm at 1 kW using a tantalum target, argon as a carrier gas, and controlled additions of nitrogen.

2.1. MECHANICAL PROPERTY TESTING

The elastic modulus and hardness values of the films were measured using the continuous stiffness measurement option on a Nano Indenter II^{TM} with a Berkovich diamond indenter at a superimposed excitation frequency of 45 Hz and displacement of 3 nm. All tests were conducted in ambient air at a loading rate of 0.1 s^{-1} with maximum contact (plastic) displacement ranging from 20 to 800 nm using a Berkovich indenter. Indentation loads and corresponding displacements were recorded continuously throughout each test. The area for each indentation in the as-sputtered film was determined from an area shape function derived from fused silica. These areas were then used with the slopes from the unloading curves to determine stiffness and elastic modulus following the method of Oliver and Pharr (1992). Hardness was calculated for each test from the maximum load and the area of the indentation.

2.2. FRACTURE TESTING

The resistance to interfacial fracture was determined from indentation and nanoscratch tests (Moody et al., 1998a). For the nanoindentation tests, a conical diamond indenter with a nominal 1.0 μm tip radius and a 90° included angle was driven into the films at a loading rate of 600 μN s^{-1} to maximum loads of 25, 50, 100, 200, 400 and 600 mN. During each test, the normal loads and displacements were continuously recorded. For the nanoscratch tests, a second conical diamond indenter also with a nominal 1.0 μm tip radius and a 90° included angle was simultaneously driven into the films at a loading rate of 500 μN s^{-1} and across the films at a lateral displacement rate of 0.5 μm s^{-1} until a portion of the film spalled from the substrate. During each test, the normal and tangential loads along with the normal and lateral displacements were continuously recorded.

3. Results

3.1. COMPOSITION

Scanning Auger depth profiling of the as-deposited film showed a well-defined chromium peak at the sapphire substrate interface corresponding to the chromium adhesive layer as shown in Figure 1. Aging at 400 °C for 2 hours led to through thickness migration of chromium and partial depletion of the adhesive layer. Nevertheless, the layer remained continuous. This was confirmed by backside optical examination where a thin translucent chromium layer covered the substrate interface. In contrast, long term annealing at 400 °C for 8 hours led to complete depletion of the chromium adhesive layer creating a uniform through thickness gold-chromium solid solution. Backside optical examination did not reveal any evidence of a chromium interlayer.
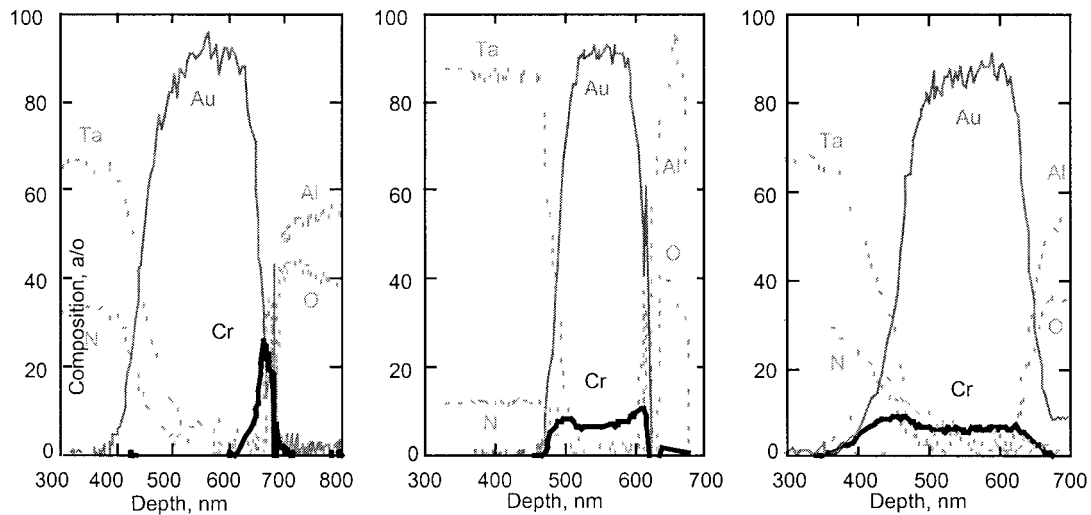
Figure 1. Composition profiles of the (a) as-deposited film, (b) the film annealed at 400 °C for 2 hours and (c) the film annealed at 400 °C for 8 hours show that diffusion during annealing has depleted the continuous chromium adhesive layer.
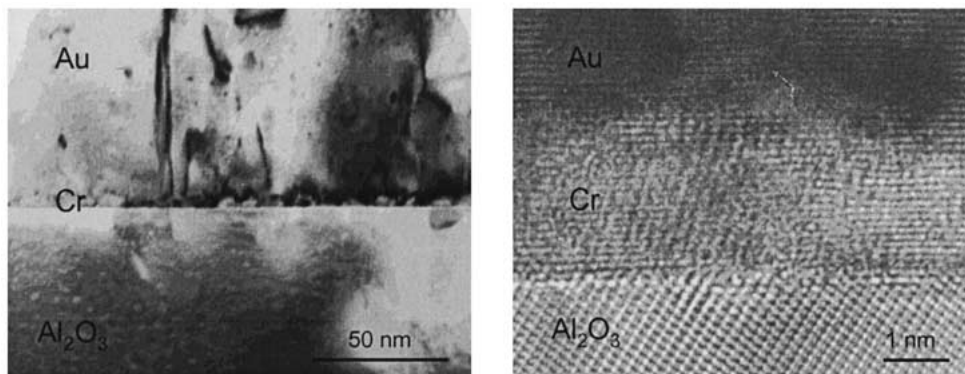
Figure 2. (a) TEM and (b) HRTEM showed that the chromium formed as islands with an epitaxial structure that coalesced to form a continuous interlayer.

3.2. STRUCTURE

The structures of the as-deposited gold-chromium films and of the films annealed at 400 °C for 8 hours are shown in Figures 2 and 3. In the as-deposited condition, the chromium formed as discrete islands that grew to form a nearly uniform 6-nm-thick film across most of the substrate interface. High Resolution TEM showed that these islands deposited epitaxially on the sapphire substrate creating a well-defined interface with little evidence of disorder. 200 nm of gold was then deposited onto the chromium layer. The gold grains were essentially equiaxed in structure with significant through thickness twinning. Figure 3 clearly shows that no adhesive layer remained in the gold on chromium films annealed at 400°C for 8 hours. Particularly noticeable is the loss of registry across the substrate interface that characterized the epitaxial structure created by chromium deposition. In-situ energy dispersive spectroscopy was then employed to determine where the chromium had migrated and its effect on film composition. The results are superimposed on the film structure and show that the chromium
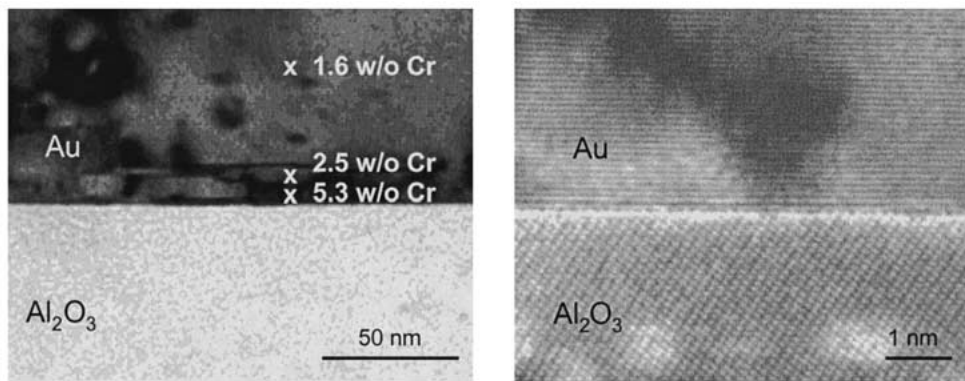
Figure 3. (a) TEM shows that annealing depleted the chromium interlayer but left chromium in solution. (b) HRTEM shows there were no reaction products or evidence of epitaxial structure along the film-substrate interface.

concentration rapidly decreased from 5 w/o along the interface to 1.6 w/o three-quarters of the way through the film. Although the concentration of chromium along the interface is likely higher than the beam-averaged value, it is not sufficient to form a continuous monolayer. EDS also showed no evidence of chromium segregation along the grain boundaries.

The structure and stresses within the tantalum nitride overlayers were characterized using a Rigaku X-ray Diffraction system with a thin film detection system and Cu-Kα radiation. The patterns showed a randomly oriented polycrystalline structure for these overlayers, typical for sputter-deposited tantalum nitride. Shifts in the 2θ peak positions for (101), (110) and (211) planes indicated significant out-of-plane strain and were used to calculate an in-plane residual compressive stress of -2.5 ± 0.6 GPa stress assuming isotropic elasticity (Moody et al., 1998b; Sun et al., 1975; Cullity, 1956). This value varied between films but was always within one standard deviation of the average.

3.3. PROPERTIES

Nanoindentation showed that the elastic modulus of all films near 115 GPa, slightly higher than average values for bulk gold. The hardness was near 2.7 GPa for all three film systems. These values are similar to those measured in sputter deposited gold films. (Moody et al., 2000; Volinsky et al., 2002a). Following the work of Tabor (1948) the corresponding yield strengths are near 900 MPa. These values are significantly higher than for bulk gold but consistent with values in films of similar thickness (Leung and Nix, 1999).

3.4. FRACTURE

In previous work (Moody et al., 2000), deposition of the tantalum nitride overlayers triggered extensive delamination and telephone cord blistering in an as-deposited gold film sample and in isolated regions on a gold-chromium film sample. The blistered material readily spalled away exposing the lower fracture surface. High resolution SEM coupled with energy dispersive spectroscopy revealed that fracture had occurred along the film-sapphire interface. The freshly exposed sapphire surfaces under the telephone cord and the circular blisters were visually smooth at 50 kX and showed no evidence of gold or chromium indicating that fracture occurred by interfacial decohesion (Reimanis et al., 1990, 1991).
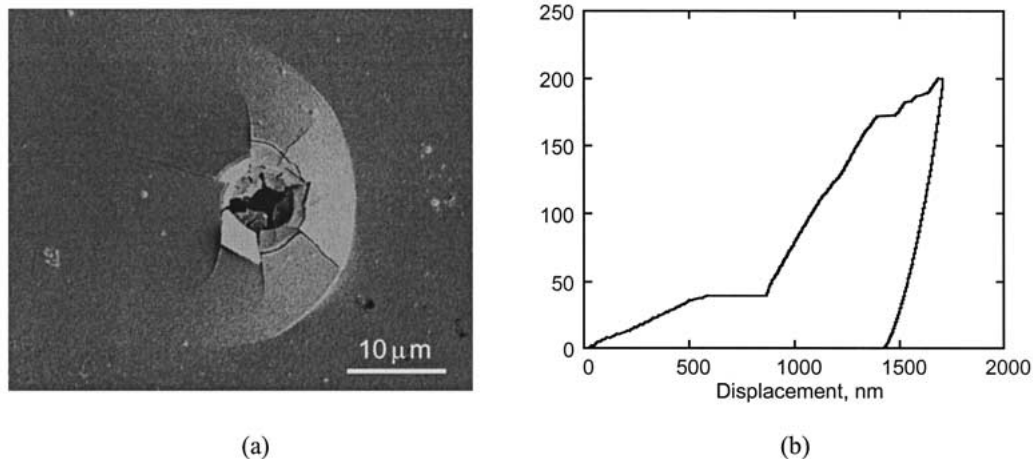
Figure 4. (a) Nanoindentation triggered circular blister formation in the as-deposited film sample. (b) The onset of fracture is readily defined by the large excursion of the load-displacement curve at relatively low loads. The short excursions at high loads correspond to small spurts of crack growth.

Additional stress from nanoindentation was required to induce interfacial fracture in the as-deposited and the annealed gold-chromium films in this study where telephone cord blistering did not occur. Fracture in the as-deposited film samples occurred in all tests where the maximum loads exceeded 25 mN, producing large circular spalls as shown in Figure 4a. The onset of fracture is defined by the rapid excursion of the indenter through the films to the sapphire substrate at essentially constant load as shown in Figure 4b. In all cases, fracture occurred by reverse or double buckle formation during indentation with the material under the indenter pinned to the substrate (Moody et al., 1998). Increased loading led to additional but smaller excursions, as shown in Figure 4b and larger blister diameters. Eventually annular cracks formed around the indenter at maximum blister height and at the furthest reaches of crack advance where the growing crack kinked in the films.

The partially and fully annealed films exhibited similar behavior but at higher loads. In addition, blister sizes were smaller and the load excursions were less pronounced. The differences were particularly noticeable in the fully annealed sample where significant scatter characterizes the loads at fracture. Fracture in the as-deposited and partially annealed films occurred along the chromium sapphire interface with no evidence of chromium left on the substrate surfaces. In contrast, fracture in the fully annealed sample occurred along the tantalum nitride-gold interface, in the gold film, and in isolated cases along the gold sapphire interface.

Determining the effects of chromium in solution on adhesion of the fully annealed films required forcing fracture to occur only along the film-sapphire interface. Previous work has shown that nucleation of interfacial fracture occurs much more readily under the shear forces than under the normal forces prevalent in indentation tests (Mattox, 1973). We therefore ran a series of 15 nanoscratch tests, where shear forces dominate, on the fully annealed samples in an effort to force interfacial failure along the sapphire substrate interface. Three of these tests triggered delamination of the gold-on-sapphire interface and formation of uniform width blisters These blisters ran back along the scratch tracks as shown in Figure 5.
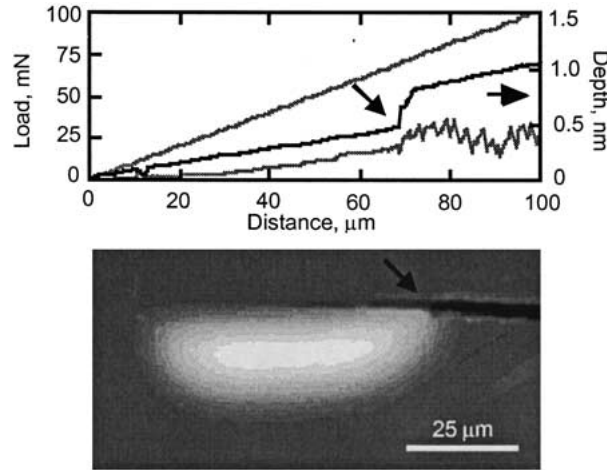
Figure 5. Nanoscratch tests promoted crack nucleation along the gold-chromium interface and subsequent blister formation.

4. Fracture analysis

The circular and uniform width blisters provide the data from which interfacial fracture energies were obtained using solutions for film systems where residual stresses dominate fracture behavior. These solutions were originally derived for single layer film-on-substrate systems (Marshall and Evans, 1984; Evans and Hutchinson, 1984; Hutchinson and Suo, 1992). Work by Bagchi et al. (1994, 1996) and more recently by Kriese et al. (1999) extended these solutions to multilayer systems by treating the multilayer film as a single layer film of the same total thickness with a transformed moment of inertia.

4.1. INDENTATION FRACTURE

In all nanoindentation tests, indentation triggered circular blisters with a pinned center giving rise to a reverse or double buckle configuration. For small buckling deflections, Marshall and Evans (1984) and Evans and Hutchinson (1984) derived an asymptotic solution for strain energy release rate by modeling the blister as a clamped circular plate with a radius much greater than the film thickness and subject to an equibiaxial compressive stress. These stresses are composed of residual stresses in the film system and stresses from nanoindentation. Assuming a rigid substrate and that all material displaced during indentation goes into the film, the stress from indentation is given as (Marshall and Evans, 1984; Evans and Hutchinson, 1984; Hutchinson and Suo, 1992),

$$\sigma_V = \frac{\overline{E}V}{2\pi(1-\bar{\nu})a^2 h},$$
(1)

where h, E and ν are the multilayer film thickness, weighted elastic modulus, and weighted Poissons' ratio respectively. ΔV is the volume of material displaced into the film. Previous work on tantalum nitride films (Moody et al., 1998) and recent work on gold-2w/o-Cu films (Moody et al., 2002) shows that approximately 60 percent of displaced indent volume is compressed into the film and contributes to in-plane stresses.

For blisters to form during indentation, the total stress from indentation and residual stresses must exceed the stress for delamination, σ_c, is given as follows (Marshall and Evans, 1984; Evans and Hutchinson, 1984; Hutchinson and Suo, 1992),

$$\sigma_c = \frac{k}{Bha^2}\left\lfloor\frac{E_{Au}}{(1 - v_{Au}^2)}\right\rfloor(I_T),\tag{2}$$

where the constant k equals 42.67 for a pinned circular clamped plate. I_T is the transformed moment of inertia for the multilayer film system (Kriese et al., 1999), v_{Au} is Poisson's ratio for gold, E_{Au} is the elastic modulus for gold, a is the blister radius, h is the total film thickness, and B is the unit width, which cancels when multiplied by the transformed moment of inertia (Kriese et al., 1999).

Following the analyses of Marshall and Evans (1984) and Evans and Hutchinson (1984), the strain energy release rate for formation of a circular blister, $\Gamma(\psi)$, is given by

$$\Gamma(\psi) = \frac{(1 - \bar{v}^2)h\sigma_v^2}{2\bar{E}} + (1 - \alpha)\frac{(1 - \bar{v})h\sigma_r^2}{\bar{E}} - (1 - \alpha)\frac{(1 - \bar{v})h(\sigma_v - \sigma_c)^2}{\bar{E}},\tag{3}$$

where $\alpha = 1 - [1 + 0.902(1 - v)]^{-1}$ (Hutchinson and Suo, 1992), h, $\bar{E}$ and $\bar{v}$ are the multilayer film thickness, weighted elastic modulus, and weighted Poissons' ratio respectively, σ_c is the stress for delamination modified for the multilayer film, and σ_r is the average residual stress in the film system (Kriese et al., 1999).

4.2. Uniform width blisters

Failure during nanoscratch testing of the fully annealed gold-chromium film system occurred by formation of uniform width blisters. The uniform width blister is modeled as a wide, clamped Euler column of width $2b$. For a blister to form between the multilayer film and substrate, the compressive residual stress, σ_r, must exceed the stress for interfacial delamination, σ_b, as follows (Hutchinson and Suo, 1992; Kriese et al., 1999)

$$\sigma_b = \frac{\pi^2}{Bhb^2}\left\lfloor\frac{E_{Au}}{(1 - v_{Au}^2)}\right\rfloor(I_T).\tag{4}$$

In this expression, b is the blister half-width. The residual stress and stress for delamination were then used to determine the strain energy release rate for interfacial fracture along the straight side wall portions of the blisters,

$$\Gamma(\psi) = \left\lfloor\frac{(1 - \bar{v}^2)h}{2\bar{E}}\right\rfloor(\sigma_r - \sigma_b)(\sigma_r + 3\sigma_b),\tag{5}$$

where σ_b is the stress for delamination modified for the multilayer film.

4.3. Interfacial fracture

The fracture energies for circular and uniform width blisters are mixed mode values consisting of shear and normal contributions. It is the normal contribution that is critical to understanding mechanisms controlling susceptibility to interfacial fracture as interfacial fracture is often a mode I failure (Hutchinson and Suo, 1992; Evans et al., 1990). However, the relationships that provide absolute values for mode I and mode II contributions are not well-defined. Of the criteria proposed,
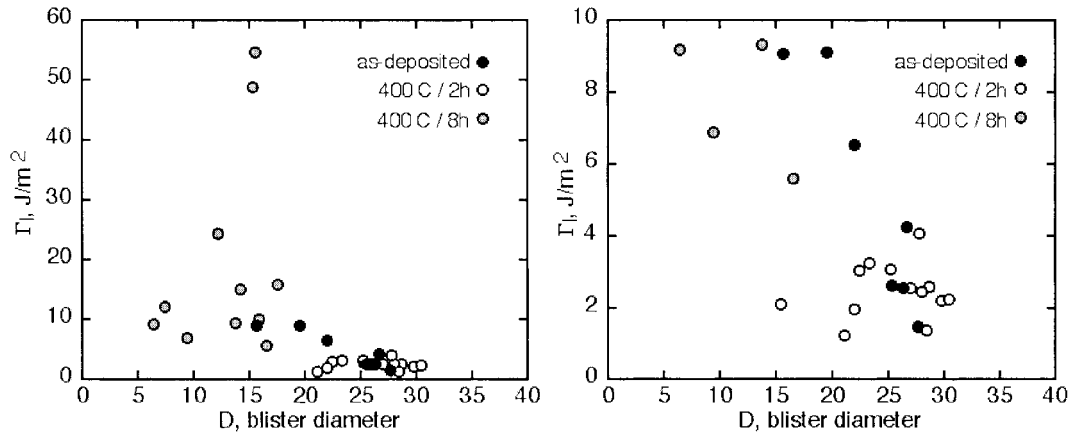
Figure 6. (a) The mode I indentation fracture energies are plotted as a function of blister diameter. (b) An expanded view of the data shows that as-deposited and partially annealed film fracture energies are similar.

$$\Gamma_I = \Gamma(\psi)\Big/ \Big\lfloor 1 + \tan^2\{(1 - \lambda)\psi\}\Big\rfloor \qquad (6)$$

is used most often (Hutchinson and Suo, 1992; Thouless et al., 1992). In this equation, λ is a material parameter equal to 0.3 for most materials, and ψ is the phase angle of loading. The phase angle of loading is determined from numerical solutions (Hutchinson and Suo, 1992) based on an effective loading parameter, σ_r/σ_c, back-calculated from the fracture energy (Moody et al., 1998).

5. Discussion

Equations (1)–(3) and (6) were used to calculated fracture energies from indentation induced blisters in the as-deposited and annealed films systems. The fracture energies were calculated from loads at the onset of the last load excursion in each test assuming this corresponds with the full extent of fracture. It should be noted that we could not factor out contributions to fracture energy from annular and radial cracking. However, comparison with test results where the extent of radial and annular cracking varied markedly show that these contributions were not significant.

The mode I indentation fracture energies are plotted in Figure 6 as a function of blister diameter. Figure 6b is an expanded view of the data showing the measured fracture energies for the as-deposited film and the film annealed at 400 °C for 2 hours approach a lower limiting value. Figure 7 presents the fracture energies as a function of blister diameter normalized with respect to indentation diameter at the point of the last excursion. Plotting data in this manner shows that the large increase in fracture energy at the small blister sizes results from crack tip plastic zone interactions with the plastic zone created under the indenter (Volinsky et al., 1999, 2002a). It also reveals two trends in behavior that depend on the fracture path. When fracture occurs cleanly along the substrate interface, there is much less interaction between crack tip and indenter plastic zones than when fracture occurs through the gold film and along the overlayer-gold film interface. This parallels the relationship between fracture energies and failure modes Volinsky et al. (2002b) observed in low-k dielectric films and supports the conclusion that plastic zone interactions have a strong effect on measured fracture energies even for relatively large blisters. At very large blister sizes, the lower limit represents values
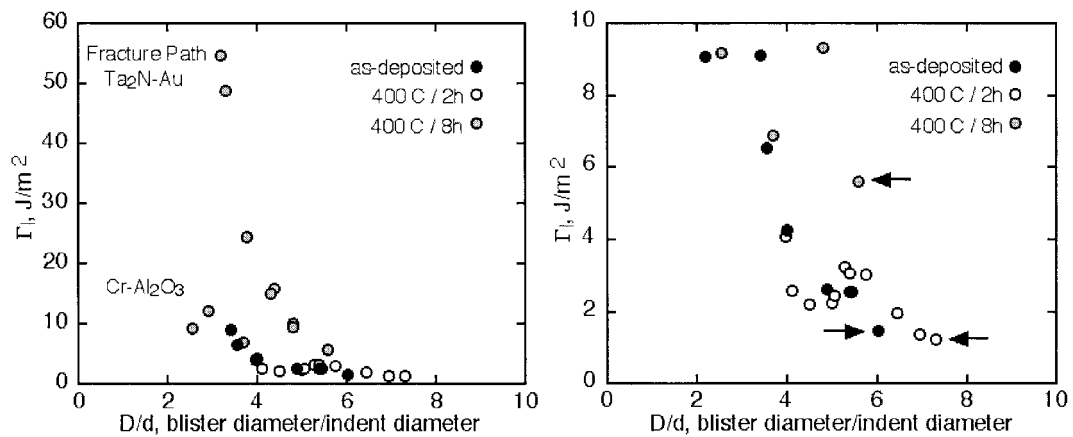
Figure 7. Plotting fracture energies as a function of normalized blister diameter indicates that the large increase in fracture energy at the small blister sizes results from crack tip plastic zone interactions with the plastic zone created by the indenter.
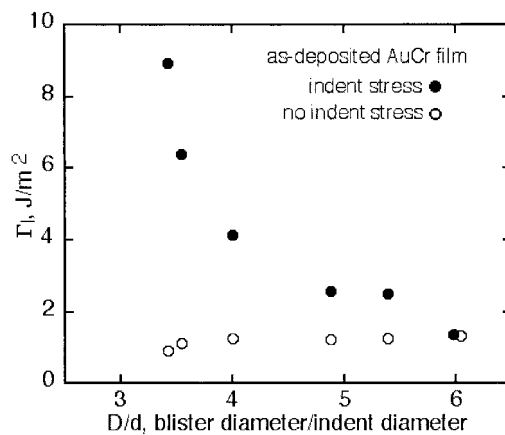

Figure 8. The fracture energies calculated with and without indentation contributions shows that the lower limit reached at the largest blister diameter for the as-deposited sample corresponds to the interfacial fracture energy.

where crack tip-indenter interactions no longer have a significant effect on measured fracture energies.

The fracture energies were also calculated without indentation contributions for comparison. This data is shown in Figure 8 for the as-deposited sample along with fracture energies calculated with indentation contributions. This figure clearly shows that the lower limit reached at the largest blister diameter for the as-deposited sample corresponds to the interfacial fracture energy. The same behavior was observed for the sample annealed at 400 °C for 2 hours. This comparison identifies the weakest bonded region of the film. It also represents the conservative limit for sample adhesion for assessing performance and reliability and for design.

Fracture energies are also given in Table 1 along with blister widths and diameters, delamination stresses, residual stresses, and phase angles of loading. The data for the as-deposited and partially annealed films correspond to lower limiting values while the data for the fully annealed film is from the largest blister. Values from previous work on as-deposited gold and gold-chromium films where deposition of stressed overlayers triggered telephone cord

Table 1. Fracture energy results for as-deposited gold, gold-chromium films, and annealed gold-chromium films.

Film	h_{Au} (nm)	$h_T a_2 N$ (nm)	$2b, 2c$ (μm)	σ_b, σ_c (μm)	σ_r (GPa)	$\Gamma(\psi)$ (J m^{-2})	ψ	Γ_I (J m−2)	Fracture path
Stressed overlayer									
Au-AD	200	275	28.8	0.3	−1.4	1.3	−75	0.5	Au-Al$_2$O$_3$
Au-Cr-AD	200	450	57.8	0.1	−1.8	2.9	−82	0.9	AuCr-Al$_2$O$_3$
Nanoindentation									
Au-Cr-AD	200	450	27.7	1.7	−1.7	2.6	−63	1.3	AuCr-Al$_2$O$_3$
400 °C/2h	200	490	28.4	1.9	−2.0	2.2	−60	1.2	AuCr-Al$_2$O$_3$
400 °C/8h	200	490	16.6	4.1	−2.0	13.2	−71	5.5	Ta$_2$N-Al$_2$O$_3$, Au, AuCr-Al$_2$O$_3$
Nanoscratch									
400 °C/8h	200	490	24.5	0.6	−2.0	3.1	−71	1.3	AuCr-Al$_2$O$_3$

blistering are also included in Table 1 (Moody et al., 2000). This work clearly showed that chromium interlayers enhanced gold film adhesion.

Table 1 shows that as-deposited film indentation fracture energies are slightly higher than values obtained from telephone blisters on the same film. This is consistent with the observation that the portion of the as-deposited film, which did not exhibit telephone cord blistering is more strongly adhered to the substrate. Fracture energies measured in the partially annealed film were similar, as expected for a continuous chromium interlayer. When fully annealed, the average fracture energy increased dramatically. This increase can be attributed to a change in fracture path from along the substrate interface to a mixed mode of fractures along the overlayer-gold interface, within the gold, and in isolated instances along the substrate interface.

Following indentation testing, nanoscratch tests were used to force fracture occur along the substrate interface in the fully annealed samples. The fracture energies from these tests were determined using Equations (4)–(6) and are given in Table 1. Under these conditions, the fracture energies in fully annealed samples equaled values measured in partially annealed films, even though the film systems had markedly different compositions and structures. The partially annealed films had a continuous chromium adhesive layer between the gold and sapphire substrate whereas diffusion had reduced the fully annealed films to a solid solution of gold and chromium. These results clearly show that chromium in solution is as effective in promoting adhesion as continuous chromium adhesive layers. The impact on hybrid microcircuits service life is dramatic as the film adhesion and device performance do not degrade as long as chromium remains in solution along the substrate interface.

6. Conclusions

In this study, highly compressed overlayers were combined with nanoindentation to study the effects of diffusion during post deposition annealing on susceptibility to interfacial fracture of gold-chromium films used in hybrid microcircuits. The samples consisted of 200 nm of gold on 6 nm chromium multilayer films sputter deposited on polished sapphire substrates. The

thin chromium deposited epitaxially on the sapphire substrate creating a well-defined interface with little evidence of disorder. Annealing at 400 °C for 2 hours reduced the thickness of the chromium interlayer while annealing at 400 °C for 8 hours drove all chromium into solution. Stressed overlayers, nanoindentation, and nanoscratch testing were then used to trigger interfacial delamination and blister formation. Interfacial fracture energies were then determined from the blister heights and widths using mechanics-based models. The tests showed that interfacial fracture occurred in the as-deposited and annealed films at energies near 1.3 J m^{-2} even when diffusion had driven all chromium into solution. Only when fracture occurred in the gold film or along the overlayer-gold interface were energies higher. These results clearly demonstrate that chromium in solution is as effective in promoting adhesion as continuous chromium adhesive layers.

Acknowledgements

References

Bagchi, A., Evans, A.G. (1996). Measurements of the debond energy for thin metallization lines on dielectrics. *Thin Solid Films* **286**, 203–212.

Bagchi, A., Lucas, G.E., Suo, Z. and Evans, A.G. (1994). A new procedure for measuring the decohesion energy for thin ductile films on substrates. *Journal of Materials Research* **9**, 1734–1741.

Bahr, D.F., Hoehn, J.W., Moody, N.R. and Gerberich, W.W. (1997). Adhesion and acoustic emission analysis of failures in nitride films with a metal interlayer. *Acta Materialia* **45**, 5163–5175.

Cao H.C. and Evans, A.G. (1989). An experimental study of the fracture resistance of bimaterial interfaces. *Mechanics of Materials* **7**, 295–304.

Charalambides, P.G., Lund, J., Evans, A.G. and McMeeking, R.M. (1989). A test specimen for determining the fracture resistance of bimaterial interfaces. *Journal of Applied Mechanics* **56**, 77–82.

Cullity, B.D. (1956). *Elements of X-Ray Difffraction*. Addison-Wesley Publishing Co., Reading, MA.

Evans, A.G. and Hutchinson, J.W. (1984). On the mechanics of delamination and spalling in compressed films. *International Journal of Solids and Structures* **20**, 455–466.

Evans, A.G., Ruhle, M., Dalgleish, B.J., Charalambides, P.G. (1990). The fracture energy of bimaterial interfaces. In: *Metal-Ceramic Interfaces* (edited by Ruhle, M., Evans, A.G., Ashby, M.F. and Hirth, J.P.) Pergammon Press, Oxford,. 345–364.

George, M.A., Glaunsinger, W.S., Thundat, T. and Lindsay, S.M. (1990). Electrical, spectroscopic, and morphological investigation of chromium diffusion through gold films. *Thin Solid Films* **189**, 59–72.

He, M.Y., Evans, A.G. and Hutchinson, J.W. (1996). Interface cracking phenomena in constrained metal layers. *Acta Metallurgica et Materialia* **44**, 2963–2971.

Hutchinson, J.W. and Suo, Z. (1992). Mixed mode cracking in layerd materials. In: *Advances in Applied Mechanics*. (edited by Hutchinson, J. W., Wu, T. Y.), Vol. 29, Academic Press Inc., New York. NY, 63–191.

Kriese, M.D., Moody, N.R. and Gerberich, W.W. (1998). Effects of annealing and interlayers on the adhesion energy of copper thin films to SiO$_2$/Si Substrates. *Acta Materialia* **46**, 6623–6630.

Kriese, M.D., Gerberich, W.W. and Moody, N.R. (1999). Quantitative adhesion measures of multilayer films – I. Indentation mechanics. *Journal of Materials Research* **14**, 3007–3018.

Leung, O.S. and Nix, W.D. (1999). Wafer curvature studies of strengthening mechanisms in thin films on substrates. In: *Thin Films-Stresses and Mechanical Properties VIII*. (edited by Vinci, R., Kraft, O., Moody, N., Besser, P. and Shaffer, E.), Vol. 594, Materials Research Society, Warrendale, PA, 51–56.

Marshall, D.B. and Evans, A.G. (1984). Measurement of adherence of residually stressed thin films by indentation mechanics of interface delamination. *Journal of Applied Physics* **56**, 2632–2638.

Mattox, D.M. (1973). Thin film metallization of oxides in microelectronics. *Thin Solid Films* **18**, 173–186.

Mittal, K.L. (1976). Adhesion measurements of thin films. *Electrocomponent Science and Technology* **3**, 21–42.

Moody, N.R., Hwang, R.Q., Venkataraman, S., Angelo, J.E., Norwood, D.P. and Gerberich, W.W. (1998a). Adhesion and fracture of tantalum nitride films. *Acta materialia* **46**, 585–597.

Moody, N.R., Medlin, D., Boehme, D. and Norwood, D.P. (1998b). Film thickness effects on the fracture of tantalum nitride on aluminum nitride film systems. *Engineering Fracture Mechanics* **61**, 107–118.

Moody, N.R., Adams, D.P., Volinsky, A.A., Kriese, M.D. and Gerberich, W.W. (2000). In: *Interfacial Engineering for Optimized Properties II* (edited by Briant, C., Carter, C., Hall, E. and Nutt, S.), Vol. 494, Materials Research Society. Pittsburgh, PA, 195–205.

Moody, N.R., Yang, N., Adams, D.P., Cordill, M.J. and Bahr, D.F. (2002) The effects of copper on the interfacial fracture of gold films, In: *Thin Films-Stresses and Mechanical Properties IX* Vol. 695, (edited by Ozkan, C.S., Camarata, R.C., Freund, L.B. and Gao, H.) Materials Research Society, Pittsburgh, PA, L7.5.1–L7.5.6.

Munitz, A. and Komem, Y. (1976). Structural and resistivity changes in heat-treated chromium-gold films. *Thin Solid Films* **37**, 171–179.

Munitz A. and Komem, Y. (1980). The increase in the electrical resistance of heat-treated Au/Cr films. *Thin Solid Films* **71**, 177–188.

Oliver, W.C. and Pharr, G.M. (1992). An improved technique for determining hardness and elastic modulus using load and displacement sensing indentation experiments. *Journal of Materials Research* **7**, 1564.

Rairden, J.R., Neugebaur, C.A. and Sigsbee, R.A. (1971). Interdiffusion in thin conductor films-chromium/gold, nickel/gold, and chromium silicide/gold. *Metallurgical Transactions* **2**, 719–722.

Reimanis, I.E., Dalgleish, B.J., Brahy, M, Ruhle, M. and Evans, A.G. (1990). Effects of plasticity on the crack propagation resistance of a metal/ceramic interface. *Acta Metallurgica et Materialia* **38**, 2645–2652.

Reimanis, I.E., Dalgleish, B.J. and Evans, A.G. (1991) The fracture resistance of a model metal/ceramic interface. *Acta Metallurgica et Materialia* **39**, 3133–3141.

Sun, R.C., Tisone, T.C. and Cruzan, P.D. (1975). The origin of internal stress in low-voltage sputtered tungsten films. *Journal of Applied Physics* **46**, 112–117.

Suo, Z. and Hutchinson, J.W. (1989) Sandwich test specimens for measuring interface crack toughness. *Materials Science and Engineering* **A107**, 135–143.

Tabor, D. (1948). A simple theory of static and dynamic hardness. *Proceedings of the Royal Society* **A192**, 247–274.

Thomas, R.E. and Haas, G.A.J. (1972). Diffusion measurements in thin films utilizing work function changes. *Applied. Physics* **43**, 4900–4907.

Thouless, M.D., Hutchinson, J.W. and Liniger, E.G. (1992). Plane-strain, buckling driven delamination of thin films: model experiments and mode-II fracture. *Acta Metallurgica et Materialia* **40**, 2639–2649.

Volinsky, A., Tymiak, N.I., Kriese, M.D., Gerberich, W.W. and Hutchinson, J.W. (1999). Quantitative modeling and measurement of copper thin film adhesion. In: *Fracture and Ductile vs Brittle Behavior-Theory, Modeling, and Experiment* (edited by Beltz, G.E., Blumberg Selinger, R.L., Marder, M.P., Kim, K-S.), Vol. 539, Materials Research Society, Pittsburgh, PA, 277–290.

Volinsky, A.A., Moody, N.R. and Gerberich, W.W. (2002a). Interfacial toughness measurements for thin films on substrates. *Acta Materialia* **50**, 441–466.

Volinsky, A.A., Vella, J.B., Gerberich, W.W. (2002b). Fracture toughness, adhesion, and mechanical properties of low-k dielectric thin films measured by nanoindentation. *Thin Solid Films* **429**, 201–210.

Wei, Y. and Hutchinson, J.W. (1998). Interface strength, work of adhesion and plasticity in the peel test. *International Journal of Fracture* **93**, 315–333.